Electronic Supplementary Material (ESI) for RSC Advances.

Supporting Information

Side Chain Structure Affects the Molecular Packing and Photovoltaic Performance of Oligothiophene-Based Solution-Processable Small Molecules

Shang-Che Lan[1], Chiao-Kai Chang[1], Yueh-Hsin Lu[1], Shu-Wei Lin[1], Alex K-Y. Jen[2], and Kung-Hwa Wei[1] *

1. *Department of Materials Science and Engineering, National Chiao Tung University, 300 Hsinchu, Taiwan*

E-mail: khwei@mail.nctu.edu.tw

2. *Department of Materials Science and Engineering, University of Washington, Seattle, WA, USA*

Hypothetical lamellar stacking

Base on the assumption of the lamellar structure, we suspected that there are three possible packing configurations along [100] for TBTThBTh-H molecules－**Figure S1** presented their configurations. **Figure S1(a)** show that if the arrangement of TBTThBTh-H molecules along their backbone is head-to-tail, the $d_{(100)}$-spacing of lamellar structure without interdigitation is about 23 Å. Hence, this suggests that lamellar structures would contain a certain degrees of interdigitation if the $d_{(100)}$-spacing is less than 23 Å (**Figure S1(b)**). On the other hand, the arrangement of backbone also possibly adopts a ladder configuration because of there might be a secondary force between *β*-hydrogen of thiophene and electronegative atoms (e.g. N, O, and S), which is often observed in the crystals of non-alkyl- substituted oligothiophene.[1,2] For such a ladder configuration, TBTThBTh-H molecules still form interdigitated stacking but the $d_{(100)}$-spacing would be larger than 23 Å (**Figure S1(c)**). In comparing TBTThBTh-H to TBTThBTh-C4 and TBTThBTh-C8, the additional alkyl chains on central thiophenes would prevent the secondary interaction and thus increase the tendency of the head-to-tail arrangement. As a result, TBTThBTh-C4 and TBTThBTh-C8 revealed relatively smaller spacing values such as in the case of the configuration in **Figure S1(b)**. In addition, the correlation between π-π stacking forms and molecular structure is insufficiently supported by XRD data.

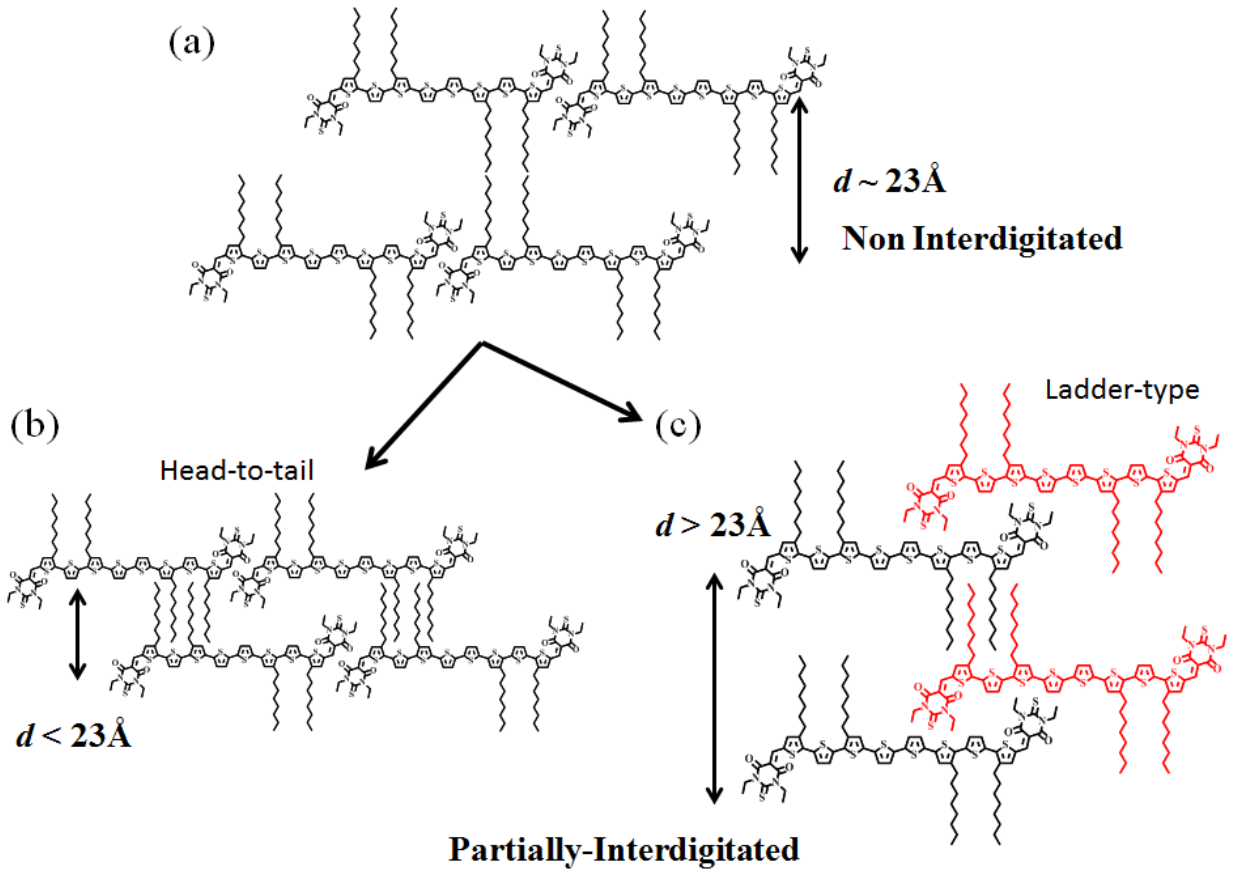

Figure S1. Three hypothetical lamellar-typed configurations of (a) non-interdigitation, (b) partial interdigitation with small spacing, and (c) partial interdigitation with large spacing for TBTThBTh-H.

CV

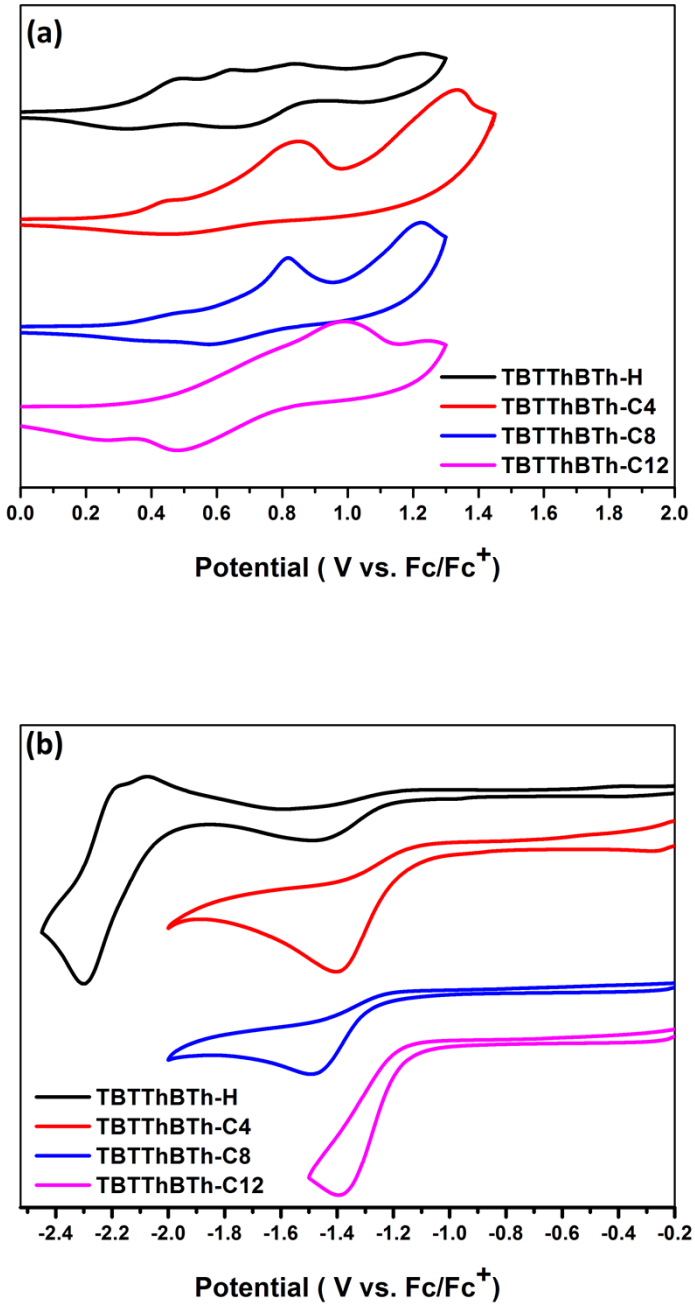

Figure S2. Cyclic voltammograms of the (a) oxidation and (b) reduction behavior for TBTThBT molecules.

XRD

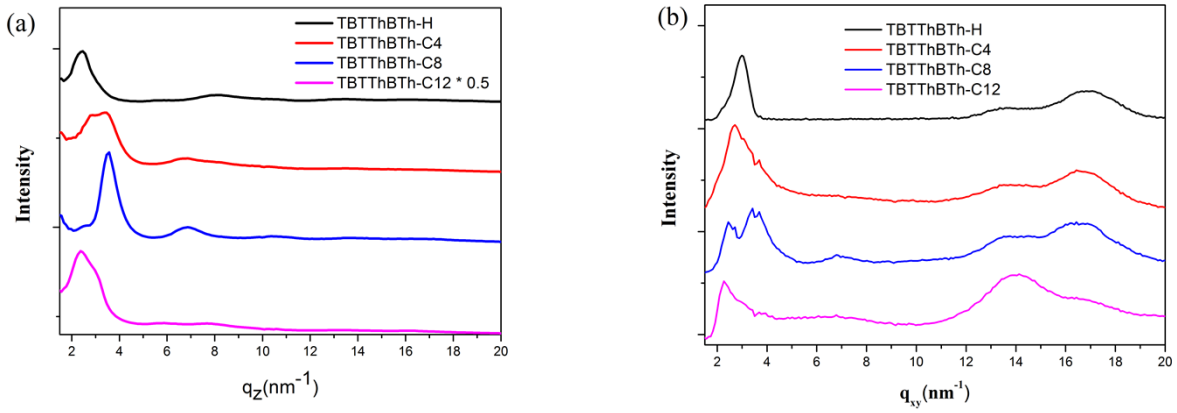

Figure S3. GIWAXS line cuts (a) out-of-plane and (b) in-plane (along the q_{xy} direction) of molecules' neat films, taken from the diffraction patterns in **Figure 4**.

Experimental Methods

Materials. Scheme 1 illustrates the general synthetic route for four molecules. Most reactions, expecting for bromination, were performed under nitrogen atmosphere. Anhydrous solvents were dried over appropriate agents, and then distilled for use. 5′′-Bromo-3,3′′-dioctyl-[2,2′:5′,2′′-terthiophene]-5-carbaldehyde (**1**), [3] 5,5′-bis(trimethylstannyl)-2,2′-bithiophene (**2a**)[4], and 5,5′-bis(trimethylstannyl)-3,3'-dialkyl-2,2′-bithiophene (**2b-2d**)[5] were synthesized according to literature procedures.

Synthesis of compound 3. Compound **1** and a stannyl compound were dissolved in anhydrous toluene by a molar ratio of 2.5/1, and the solution was purged with N_2 for 20 min. 5 mol% tetrakis(triphenylphosphine)palladium(0) ($Pd(PPh_3)_4$) was added into solution in one dose, and the reaction was carried on at 100 °C for 48 h. After cooling to room temperature, the solvent was evaporated under vacuum. The residue was purified through column chromatography (SiO_2; EtOAc/hexane, 1:9) to give a red solid. A small amount of CH_2Cl_2 was used to re-dissolve the solid, which was re-precipitated from MeOH to obtain the final compound.

Compound **3a**. ^{1}H NMR (300 MHz, $CDCl_3$): δ (ppm) 9.81 (s, 2H), 7.58 (s, 2H), 7.23 (d, *J* = 3.6 Hz, 2H), 7.10 (d, *J* = 3.9 Hz, 2H), 7.07 (s, 4H), 7.01 (s, 2H), 2.84–2.73 (m, 8H), 1.66 (br, 8H), 1.40–1.20 (m, 40H), 0.86 (t, *J* = 5.7 Hz, 12H). MS (MALDI-TOF): calcd for $C_{66}H_{82}O_2S_8$ $[M]^+$, *m*/*z* 1162.41; found, *m*/*z* 1162.34.

Compound **3b**. ^{1}H NMR (300 MHz, $CDCl_3$): δ (ppm) 9.84 (s, 2H), 7.60 (s, 2H), 7.25 (d, *J* = 3.6 Hz, 2H), 7.13 (d, *J* = 3.9 Hz, 2H), 7.04－6.99 (m, 4H), 2.87–2.76 (m, 12H), 1.70－1.63 (m, 12H), 1.46–1.28 (m, 44H), 0.97(t, *J* = 7.5 Hz, 6H), 0.88 (t, *J* = 5.7 Hz, 12H). MS (MALDI-TOF): calcd for $C_{74}H_{98}O_2S_8$ $[M]^+$, *m*/*z* 1274.53; found, *m*/*z* 1275.37

Compound **3c**. ^{1}H NMR (300 MHz, $CDCl_3$): δ (ppm) 9.81 (s, 2H), 7.58 (s, 2H), 7.23 (s, 2H), 7.10 (d, *J* = 3.9 Hz, 2H), 6.98 (s, 2H), 6,96 (s, 2H), 2.80－2.72 (m, 12H), 1.66 (br, 12H), 1.40－1.20 (m, 60H), 0.86 (t, *J* = 6.9 Hz, 18H). MS (MALDI-TOF): calcd for $C_{82}H_{114}O_2S_8$ $[M]^+$, *m*/*z* 1386.66; found, *m*/*z* 1386.49.

Compound **3d**. ^{1}H NMR (300 MHz, $CDCl_3$): δ (ppm) 9.81 (s, 2H), 7.58 (s, 2H), 7.23 (s, 2H), 7.12 (d, *J* = 3.9 Hz, 2H), 6.98 (s, 2H), 6,96 (s, 2H), 2.84－2.72 (m, 12H), 1.66 (br, 12H), 1.40－1.20 (m, 76H), 0.86 (t, *J* = 6.9 Hz, 18H). MS (MALDI-TOF): calcd for $C_{90}H_{130}O_2S_8$ $[M]^+$, *m*/*z* 1498.78; found, *m*/*z* 1498.95.

General Procedure for Knoevenagel Condensation: A two-necked flask contained the aldehyde (0.05 mmol), pyridine (0.2 mL), 1,3-diethyl-2-thiobarbituric acid (0.5 mmol), and dry chloroform (5 mL). Then the mixture was stirred at room temperature for 12 h. After finishing the reaction, the mixture was quenched into dilute aqueous solution of hydrochloric acid, and extracted with chloroform. The organic phases were dried ($MgSO_4$) and concentrated. The residue was subjected to

quickly chromatographic purification (SiO_2; chloroform/hexane, 3:1) to give a crude compound. The isolated compound was recrystallized (toluene/isopropanol) to afford a dark desired compound.

TBTThBTh-H. ^{1}H NMR (300 MHz, $CDCl_3$): δ (ppm) 8.54 (s, 2H), 7.67 (s, 2H), 7.46 (d, *J* = 3.9 Hz, 2H), 7.14 (d, *J* = 4.2 Hz, 2H), 7.06 (s, 4H), 7.01 (s, 2H), 4.62–4.52 (m, 8H), 2.84 (t, *J* = 7.5 Hz, 4H), 2.77 (t, *J* = 7.2 Hz, 4H), 1.70–1.65 (m, 8H), 1.40–1.22 (m, 52H), 0.87–0.83 (m, 12H). MS (MALDI-TOF): calcd for $C_{82}H_{102}N_4O_4S_{10}$ $[M]^+$, *m*/*z* 1526.51; found, *m*/*z* 1526.36.

TBTThBTh-C4. ^{1}H NMR (300 MHz, $CDCl_3$): δ (ppm) 8.59 (s, 2H), 7.71 (s, 2H), 7.50 (d, *J* = 6 Hz, 2H), 7.18 (d, *J* = 6 Hz, 2H), 7.18－7.06 (br, 2H) , 7.00 (d, *J* = 3Hz, 2H), 4.62–4.52 (m, 8H), 2.91－2.77 (m, 12H), 1.72–1.67 (m, 12H), 1.56–1.28 (m, 56H), 0.98(t, J= 6Hz, 6H), 0.87–0.83 (m, 12H). ^{13}C NMR ($CDCl_3$, 125 MHz, ppm) : δ 178.66, 161.09, 159.91, 149.69, 148.98, 148.89, 140.97, 140.69, 139.58, 134.91, 134.63, 134.47, 129.70, 129.45, 128.99, 128.75, 126.73, 126.27, 109.83, 43.94, 43.11, 32.56, 31.88, 31.86, 30.44, 30.02, 29.73, 29.65, 29.61, 29.54, 29.48, 29.42, 29.34, 29.29, 29.26, 22.67, 14.10, 13.98, 12.52, 12.39 MS (MALDI-TOF): calcd for $C_{90}H_{118}N_4O_4S_{10}$ $[M]^+$, *m*/*z* 1638.64; found, *m*/*z* 1638.98.

TBTThBTh-C8. ^{1}H NMR (300 MHz, $CDCl_3$): δ (ppm) 8.56 (s, 2H), 7.68 (s, 2H), 7.48 (d, *J* = 4.2 Hz, 2H), 7.16 (d, *J* = 3.9 Hz, 2H), 6.98 (m, 4H), 4.62–4.52 (m, 8H), 2.88－2.74 (m, 12H), 1.70–1.65 (m, 12H), 1.40–1.22 (m, 78H), 0.87–0.83 (m, 18H). ^{13}C NMR ($CDCl_3$, 125 MHz, ppm) : δ 178.65, 161.06, 159.89, 149.56, 148.87, 141.49, 140.69, 139.46, 136.14, 135.87, 135.61, 134.65, 134.53, 129.09, 128.97, 126.90, 126.32, 124.63, 124.50, 109.87, 43.93, 43.10, 31.85, 30.40, 30.01, 29.72, 29.68, 29.60, 29.52, 29.44, 29.41, 29.32, 29.27, 29.25, 22.66, 14.09, 12.50, 12.38. MS (MALDI-TOF): calcd for $C_{98}H_{134}N_4O_4S_{10}$ $[M]^+$, *m*/*z* 1750.76; found, *m*/*z* 1750.31.

TBTThBTh-C12. ^{1}H NMR (300 MHz, $CDCl_3$): δ (ppm) 8.56 (s, 2H), 7.69 (s, 2H), 7.48 (d, *J* = 3.6 Hz, 2H), 7.16 (d, *J* = 3.6 Hz, 2H), 6.98 (m, 4H), 4.62–4.52 (m, 8H), 2.88－2.74 (m, 12H), 1.70–1.65 (m, 12H), 1.40–1.22 (m, 94H), 0.87–0.83 (m, 18H). ^{13}C NMR (CDCl3, 125 MHz, ppm) : δ178.68, 165.50, 161.09, 159.92, 148.90, 140.97, 140.97, 140.70, 135.03, 134.92, 134.58, 134.46, 129.72, 128.99, 128.75, 126.35, 126.28, 109.87, 43.94, 43.11, 31.92, 31.88, 31.85, 30.42, 30.02, 29.70, 29.66, 29.61, 29.56, 29.53, 29.48, 29.45, 29.42, 29.36, 29.34, 29.30, 29.26, 22.66, 14.10, 12.51, 12.39. MS (MALDI-TOF): calcd for $C_{106}H_{150}N_4O_4S_{10}$ $[M]^+$, *m*/*z* 1862.89; found, *m*/*z* 1862.48.

Device Fabrication. The photovoltaic cells had a configuration of glass/indium tin oxide (ITO)/poly(3,4-ethylenedioxythiophene):polystyrenesulfonate (PEDOT:PSS)/small molecule: fullerene/Ca/Al. ITO-coated glass was pre-cleaned with detergent, DI water, acetone, and isopropanol in an ultrasonication bath (10 min each step) and then exposed under UV/ozone for 15 min. PEDOT:PSS (ca.20nm) was spin-casted onto the substrate and then annealed at 150 °C for 15 min in air. The active layer (~100nm), prepared from a hot chloroform solution (15 mg mL^{-1}, 50 °C) containing a small molecule and fullerene with a weight ratio of 6/4, was spin-casted onto the PEDOT:PSS layer in a glove box filled with dried N_2. Finally, a 15-nm-thick Ca layer and a 100-nm-thick Al layer, for use as the counter electrode, were thermally deposited under vacuum on top of the active layer. Each device featured four cells with an effective layer area of 0.04-cm^2. Current density–voltage (*J*–*V*) curves were recorded using a Keithley 2400 source meter under simulated AM 1.5 G illumination at 100 mW cm^{-2} using a Xe lamp–based Newport 66902 150-W solar simulator as a solar simulator. A silica photodiode (Hamamatsu S1133) was employed as a standard to confirm the light intensity.

The Instruments for Molecular Characterization. 1H Nuclear magnetic resonance (NMR) spectra were carried on a Burker DRX-300 NMR spectrometer. Chemical shifts are reported relative to the solvent signal. Mass spectra were determined through matrix-assisted laser desorption/ionization

time-of-flight mass spectrometry (MALDI-TOF MS), recorded using a Bruker Autoflex III instrument. Differential scanning calorimetry (DSC) was performed using a PerkinElmer Pyris 1 apparatus; approximately 2.5 mg of the sample was analyzed at a heating rate of 5 °C min^{-1}. UV–Vis absorption spectra were recorded using a Hitachi U-4100 spectrophotometer. Solid films were spin-coated from chloroform solutions (10mg /mL) onto ITO-coating glass substrates covered with a 20-nm-thick PEDOT:PSS. Cyclic voltammetry (CV) was performed using a BAS 100 electrochemical analyzer and a conventional three-electrode configuration: a glassy carbon electrode as the working electrode, a Pt wire as the counter electrode, and $Ag/AgNO_3$ (0.01 M in MeCN) as the reference electrode. Tetrabutylammonium hexafluorophosphate ($Bu4NPF_6$, 0.1 M) in MeCN was used as the supporting electrolyte. The small molecules were drop-coated onto the work electrode and analysed at a scan rate of 50 mV s^{-1}. The ferrocene/ferrocenium ion (Fc/Fc^+) pair was used as the internal standard, with the assumption that the energy level of Fc is 4.8 eV below vacuum. TEM images were recorded using an FEI T12 transmission electron microscope; a low-energy electron beam (120 keV) provided sufficient contrast to distinguish the polymer- and fullerene-rich regions of the active layer in all of the samples, without the need for heavy ion staining. The thickness of the active layer of the device was measured using a Veeco Dektak 150 surface profiler. Grazing-incidence wide-angle X-ray scattering (GIWAXS) experiments were performed at the *National Synchrotron Radiation Research Center*. The samples were prepared by spin-casting solution onto silicon wafers with 20-nm-thick PEDOT:PSS.

References

1 T. M. Barclay, A. W. Cordes, C. D. MacKinnon, R. T. Oakley and R. W. Reed, *Chem. Mater.*, 1997, **9**, 981–990.

2 R. Fitzner, C. Elschner, M. Weil, C. Uhrich, C. Körner, M. Riede, K. Leo, M. Pfeiffer, E. Reinold, E. Mena-Osteritz and P. Bäuerle, *Adv. Mater.*, 2012, **24**, 675–680.

3 J. Zhou, X. Wan, Y. Liu, G. Long, F. Wang, Z. Li, Y. Zuo, C. Li and Y. Chen, *Chem. Mater.*, 2011, **23**, 4666–4668.

4 D. Chen, Y. Zhao, C. Zhong, S. Gao, G. Yu, Y. Liu and J. Qin, *J. Mater. Chem.*, 2012, 22, 14639–14644.

5 M.-C. Yuan, M.-Y. Chiu, S.-P. Liu, C.-M. Chen and K.-H. Wei, *Macromolecules*, 2010, **43**, 6936–6938.

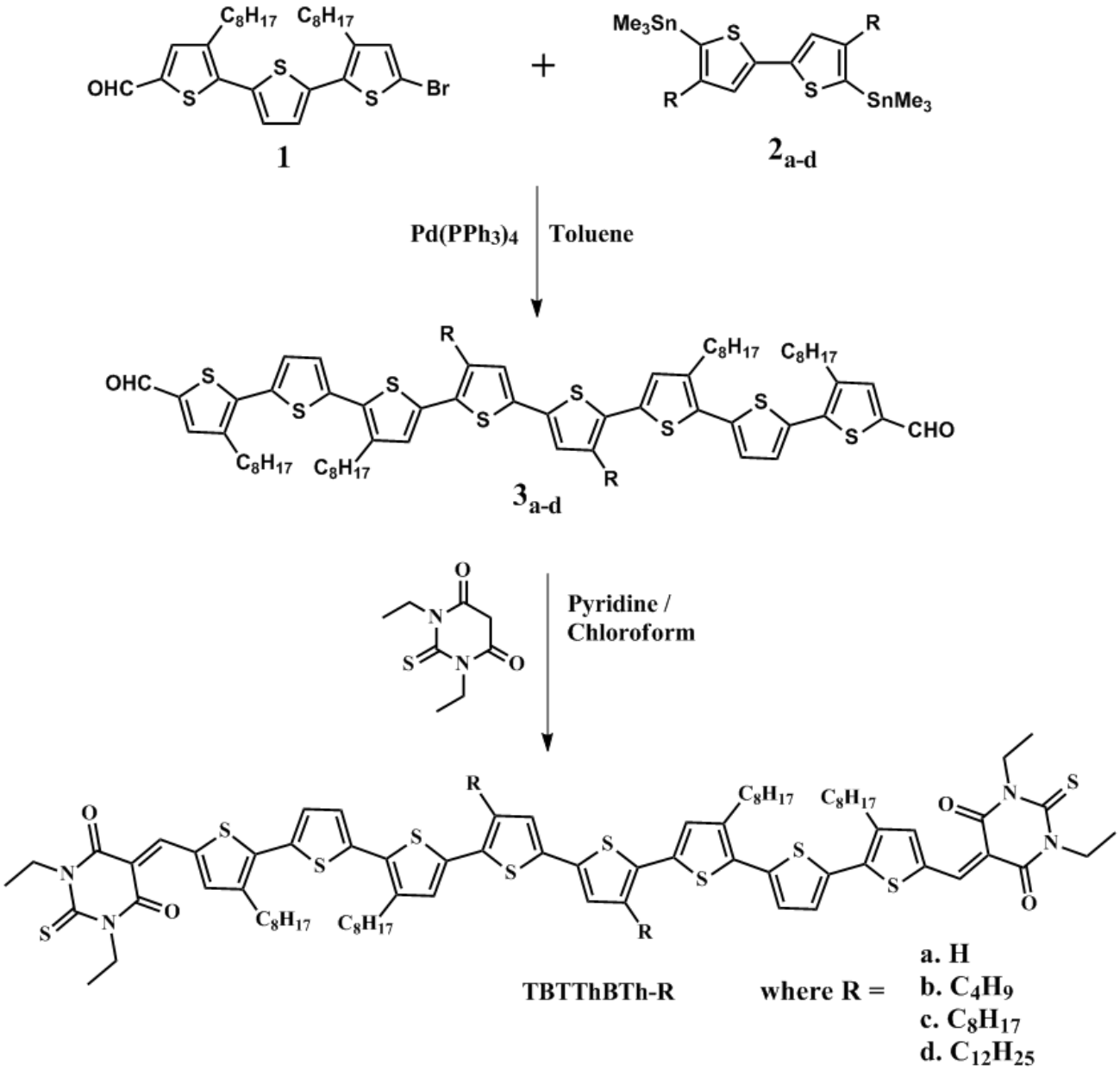

Scheme S1. General procedure for the syntheses of TBTThBTh molecules.

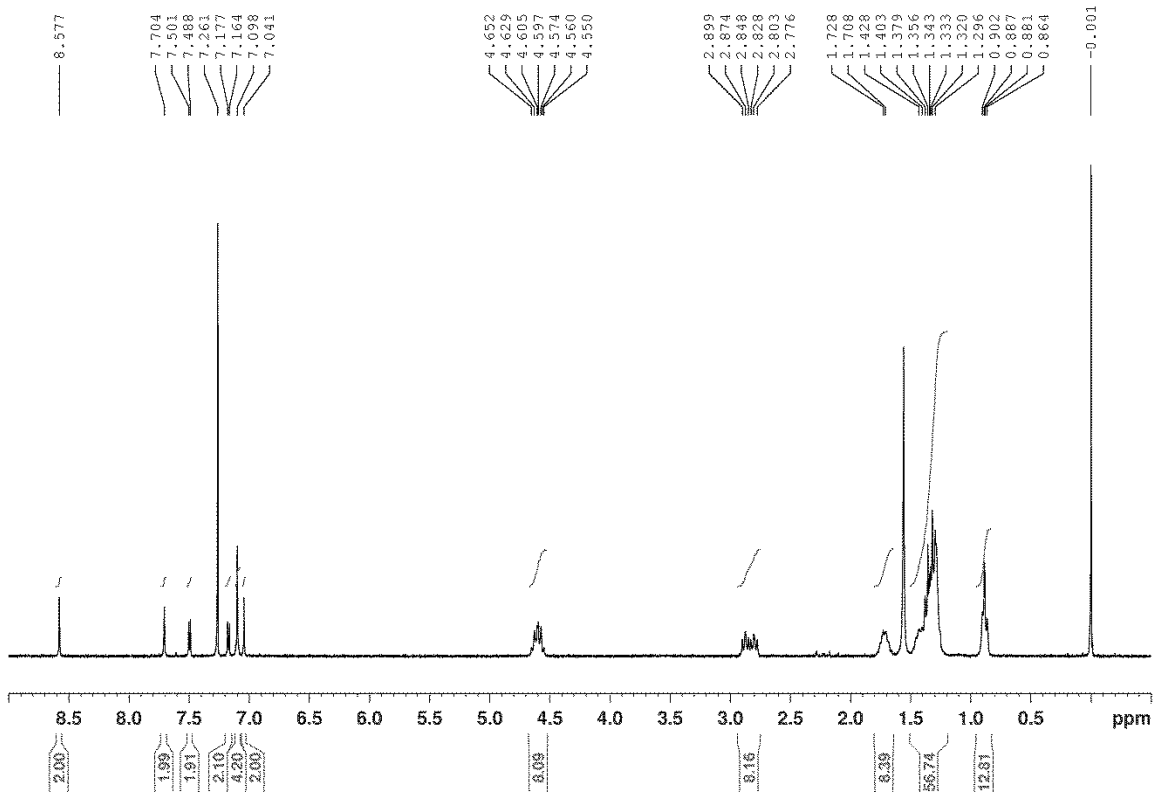

Figure S4. ^{1}H NMR spectrum of TBTThBTh-H**.**

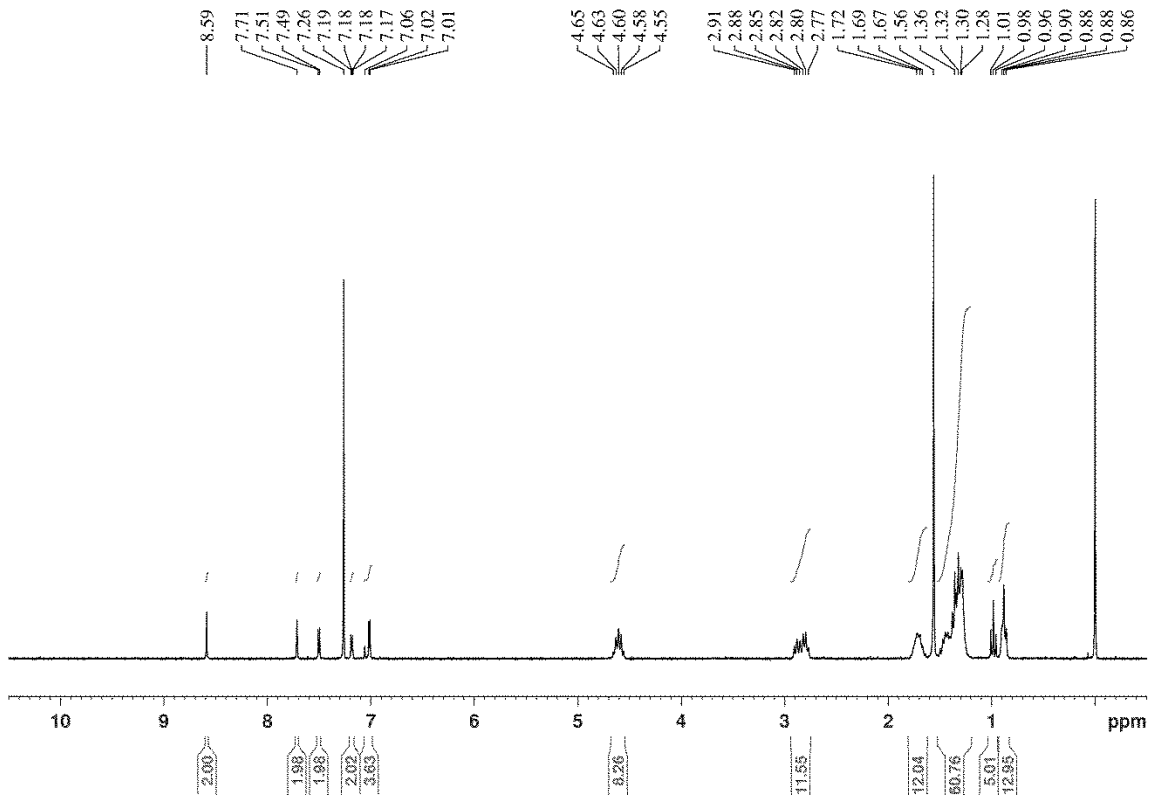

Figure S5. ^{1}H NMR spectrum of TBTThBTh-C4.

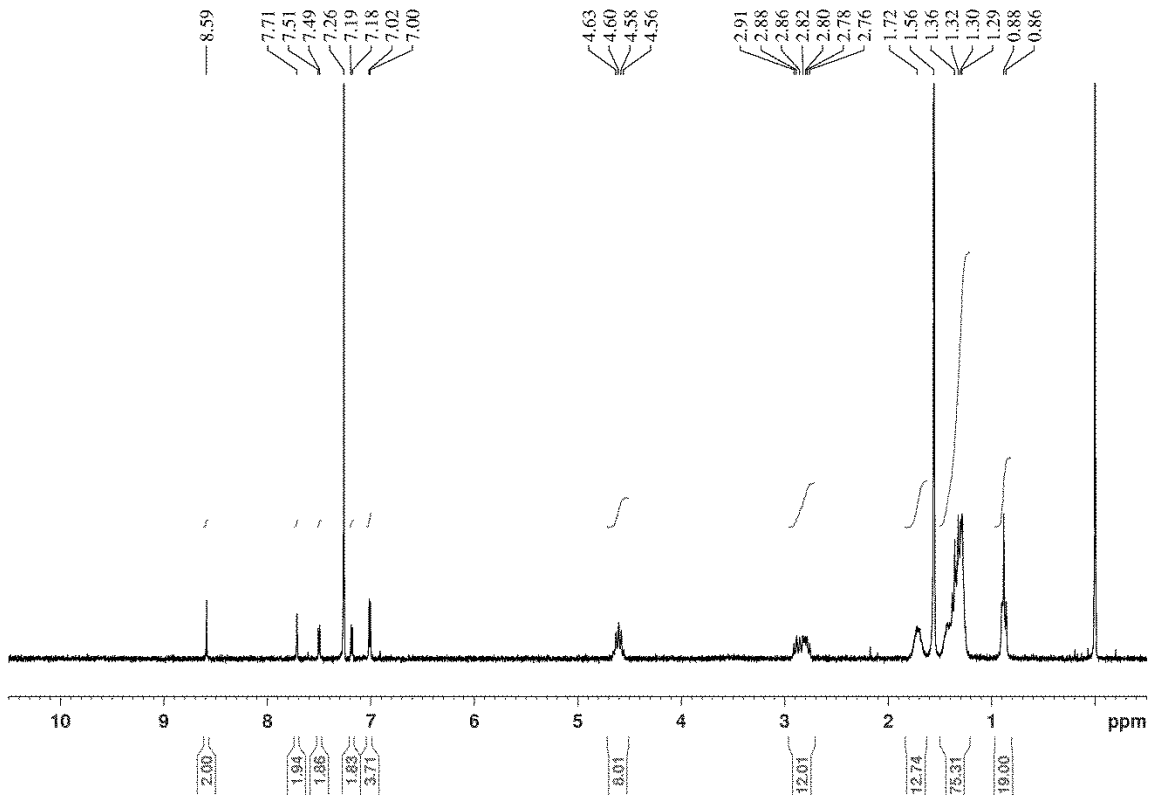

Figure S6. ^{1}H NMR spectrum of TBTThBTh-C8.

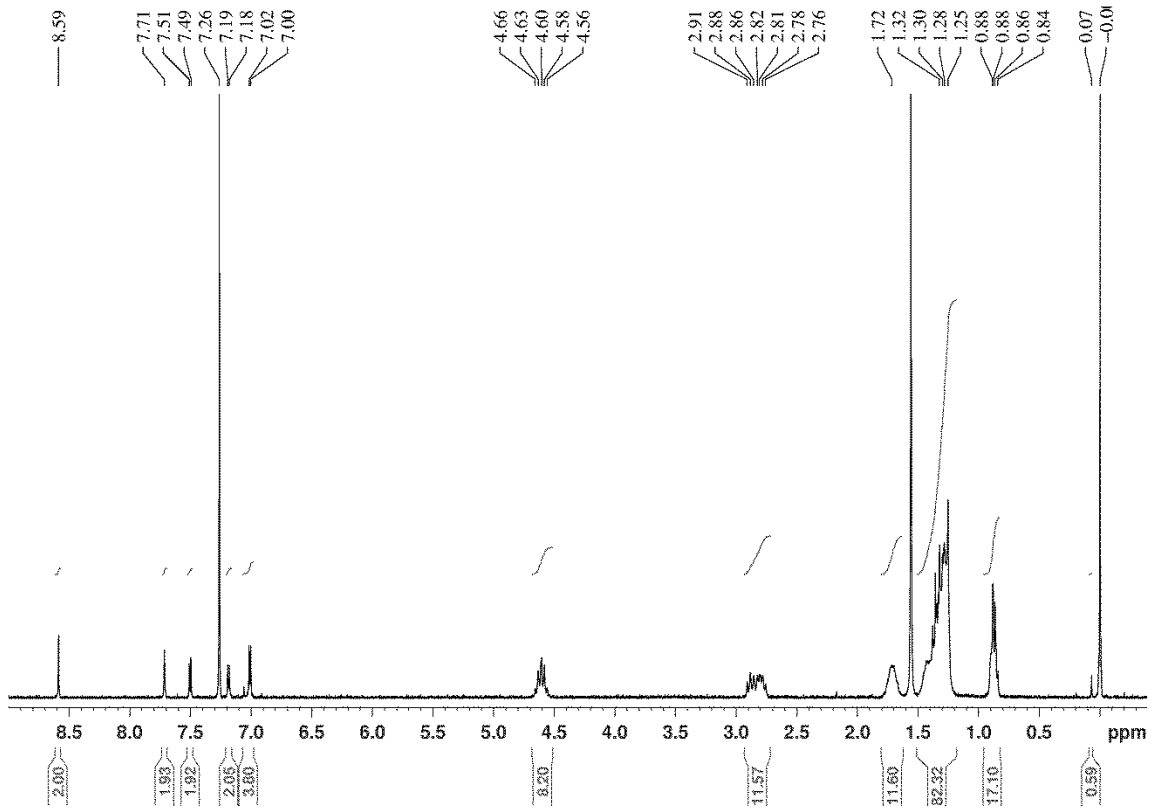

Figure S7. ^{1}H NMR spectrum of TBTThBTh-C12.

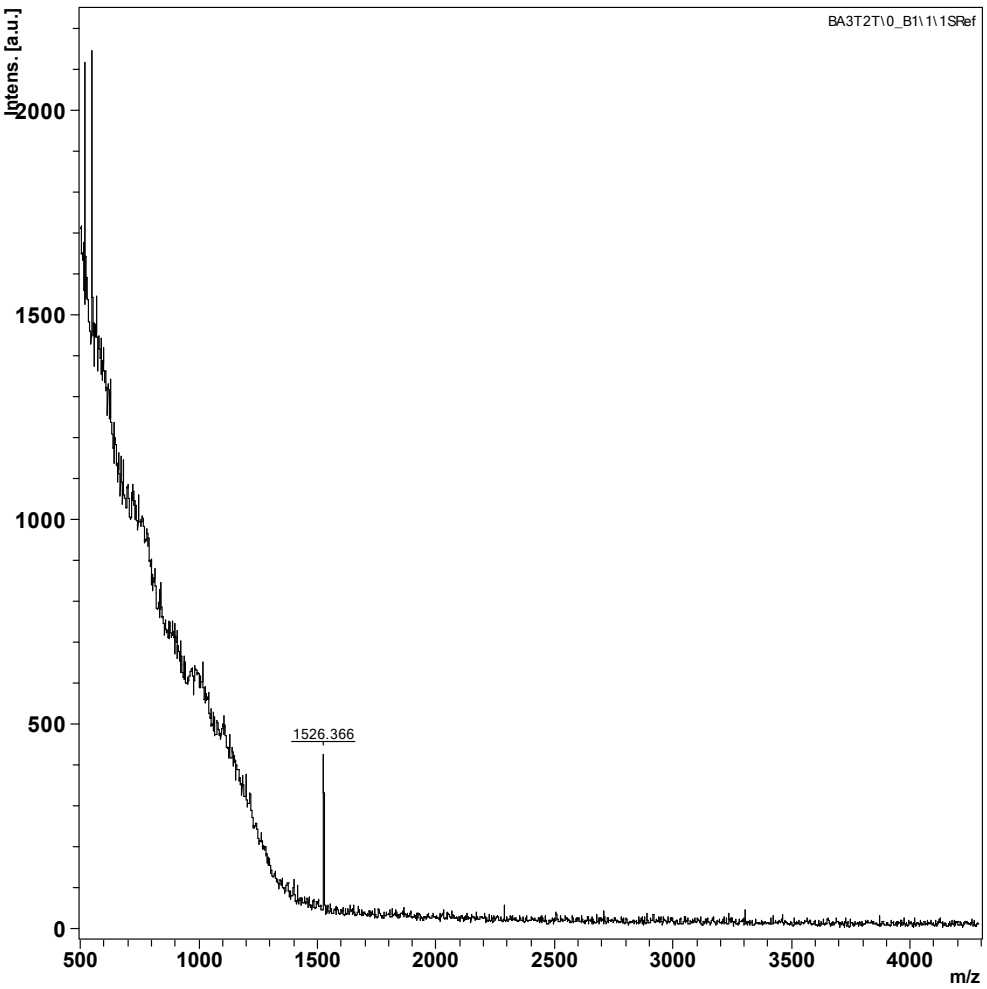

Figure S8. MALDI-TOF Mass spectrum of TBTThBTh-H.

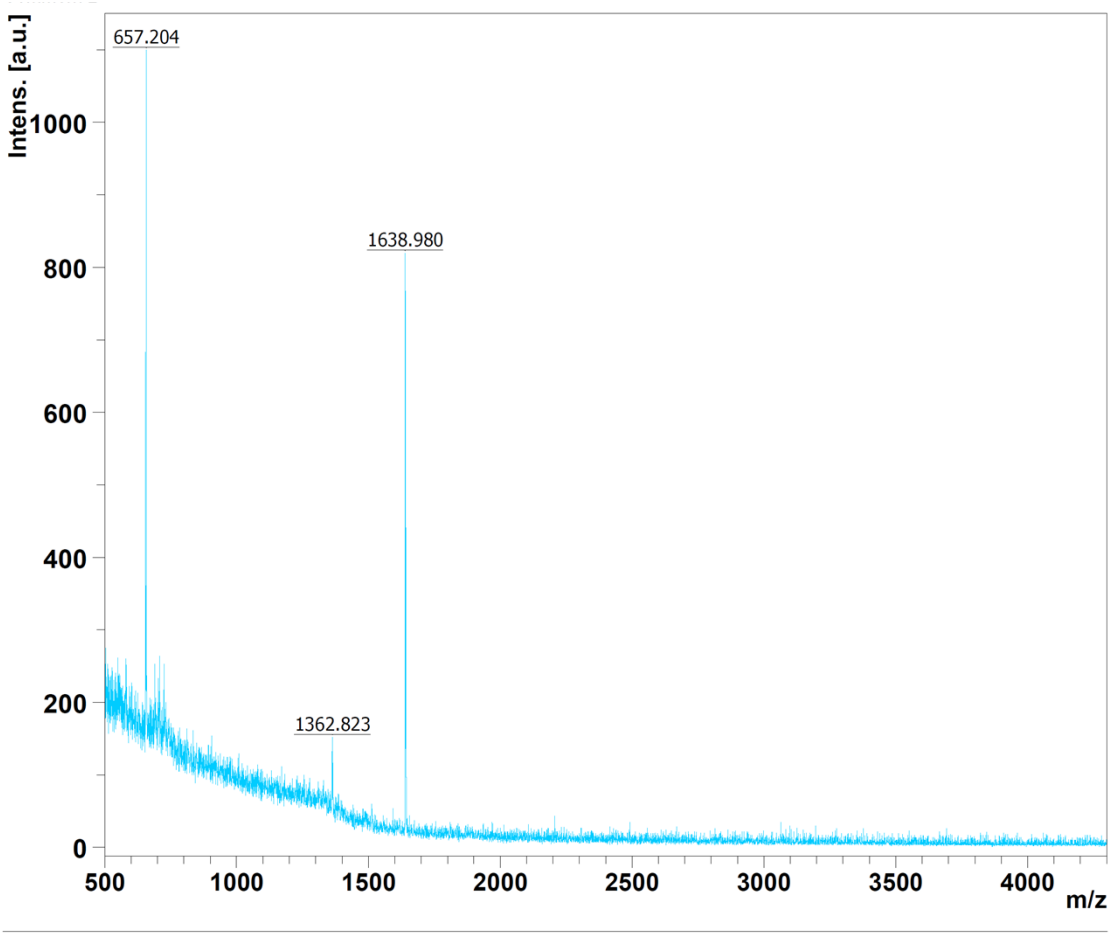

Figure S9. MALDI-TOF Mass spectrum of TBTThBTh-C4.

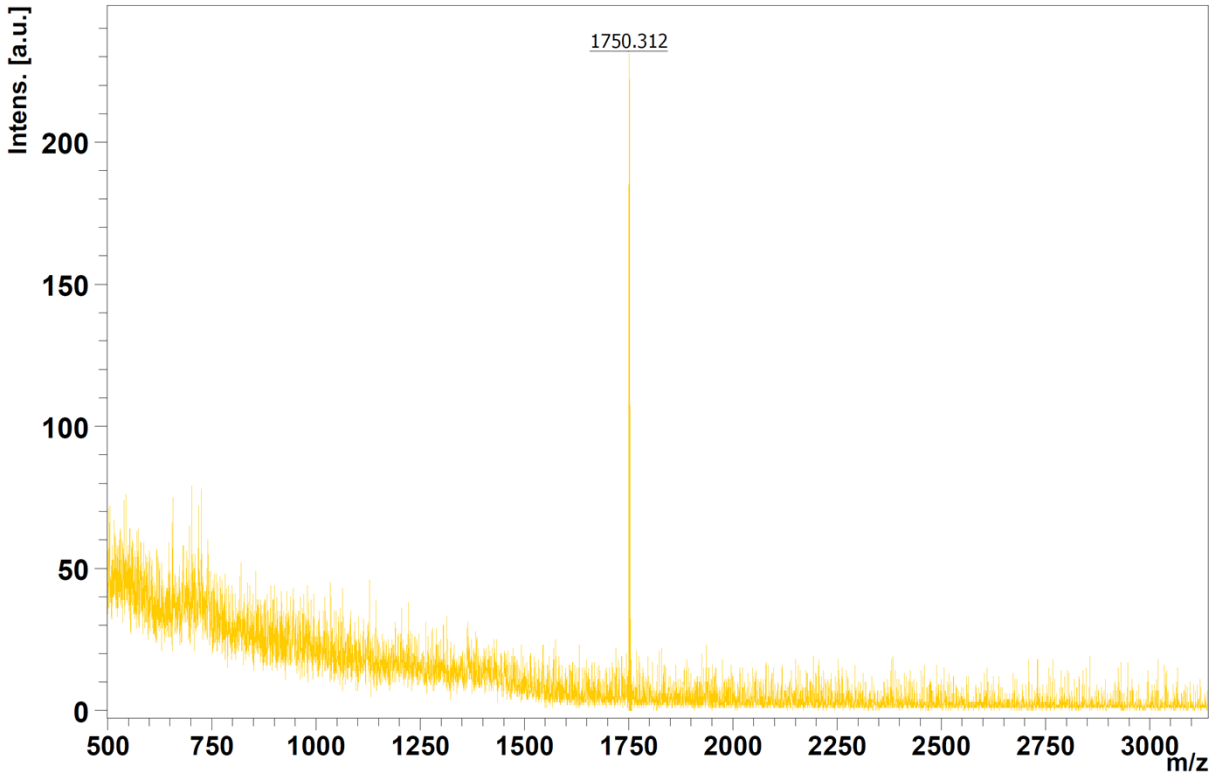

Figure S10. MALDI-TOF Mass spectrum of TBTThBTh-C8.

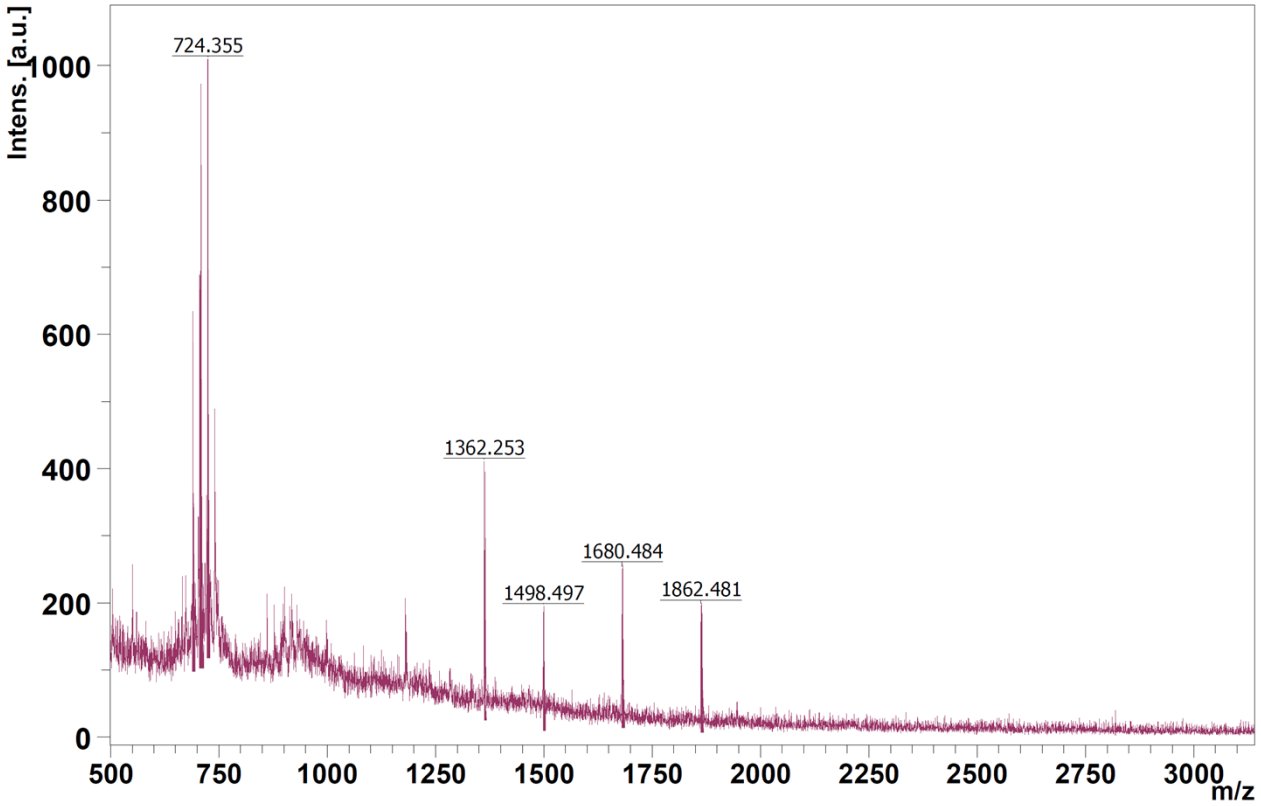

Figure S11. MALDI-TOF Mass spectrum of TBTThBTh-C12.